Synthesis, Characterization, and in Vitro Evaluation of Novel Ruthenium(II) η^6-Arene Imidazole Complexes

Carsten A. Vock,[†] Claudine Scolaro,[†] Andrew D. Phillips,[†] Rosario Scopelliti,[†] Gianni Sava,[‡,§] and Paul J. Dyson*[,†]

Institut des Sciences et Ingénierie Chimiques, Ecole Polytechnique Fédérale de Lausanne (EPFL), CH-1015 Lausanne, Switzerland, Callerio Foundation Onlus, Via A. Fleming 22-31, 34127, Trieste, Italy, and Dipartimento di Scienze Biomediche, Università di Trieste, Via L. Giorgieri 7, 34127, Trieste, Italy

Received April 27, 2006

Ten complexes of general formula [Ru(η^6-arene)Cl_2(L)], [Ru(η^6-arene)Cl$(L)_2$][X], and [Ru(η^6-arene)$(L)_3$]-$[X]_2$ (η^6-arene = benzene, *p*-cymene; L = imidazole, benzimidazole, *N*-methylimidazole, *N*-butylimidazole, *N*-vinylimidazole, *N*-benzoylimidazole; X = Cl, BF_4, BPh_4) have been prepared and characterized by spectroscopy. The structures of five representative compounds have been established in the solid state by single-crystal X-ray diffraction. All the new compounds were assessed by the same in vitro screening assays applied to [imidazole-H][*trans*-$RuCl_4$(DMSO)(imidazole)] (NAMI-A) and [Ru(η^6-arene)Cl_2(1,3,5-triaza-7-phosphaadamantane)] (RAPTA) compounds. It was found that the new compounds show essentially the same order of cytotoxicity as the RAPTA compounds toward cancer cells. Several of the compounds were selective toward cancer cells in that they were less (or not) cytotoxic toward nontumorigenic cells that are used to model healthy human cells. Thus, two of the compounds, [Ru(η^6-*p*-cymene)Cl(vinylimid)$_2$][Cl] (vinylimid = *N*-vinylimidazole) and [Ru(η^6-benzene)(mimid)$_3$][BF_4]$_2$ (mimid = *N*-methylimidazole), have been selected for a more detailed in vivo evaluation.

Introduction

The discovery of the anticancer properties of cisplatin in 1965[1,2] heralded the development of metallopharmaceuticals and founded a revolution in cancer therapy. Platinum drugs are believed to induce cytotoxicity by cross-linking DNA, causing changes to the DNA structure that inhibit replication and protein synthesis. However, the application of platinum drugs suffers from their high general toxicity, leading to severe side effects.

In comparison, ruthenium-based anticancer drugs exhibit a low general toxicity and specifically accumulate in cancer cells.[3] This is possibly due to the ability of ruthenium to mimic iron in binding to certain biomolecules, including serum transferrin and albumin, which are known to be responsible for solubilization, transport, and detoxification of iron in mammals.[3] Rapidly growing cancer cells have a greater requirement for iron, which leads to an overexpression of transferrin receptors on their surfaces such that ruthenium compounds accumulate in cancer cells.[3]

The most prominent examples of ruthenium anticancer drugs developed so far are the Ru(III) complexes Na[*trans*-$RuCl_4$(DMSO)(imid[a])], NAMI **1**, its more stable imidazolium analogue [imidH][*trans*-$RuCl_4$(DMSO)(imid)], NAMI-A **2**, and the indazole compound [indH][*trans*-$RuCl_4$(ind)$_2$], KP1019 **3** (Figure 1). Compound **2** shows high selectivity for solid tumor metastases[4,5] and low toxicity at pharmacologically active doses[6−8] and has successfully completed phase I clinical trials.[9] Metastasis control is associated with a series of biological activities that influence cell functions such as adhesion, motility, and invasion of tumor cells[10,11] because of f-actin condensation and reduction of gelatinolytic capacity.[12−14] The uniqueness of the antimetastatic effects of **2** also emerges from a comparison with other ruthenium complexes, in some cases structurally very similar to **2**, such as the imidazolium *trans*-bisimidazoletetrachlororuthenate (structurally related to **3**), which was found to be active against colorectal tumors.[15] This compound, although showing some pharmacological behaviors similar to those of **2**, is free of antimetastatic activity, and also the effects on invasion and adhesion are much less pronounced than those of **2**.[11] Compound **3** has also successfully completed phase I clinical trials.[16]

More recently, increasing interest has focused on organometallic compounds,[17−19] specifically on ruthenium(II) arene compounds which show remarkable cytotoxic properties in vitro as well as in vivo. The first complex of this kind that was evaluated for cytotoxic properties was [Ru(η^6-benzene)Cl_2-(metronidazole)] **4** (metronidazole = 1-β-hydroxyethyl-2-methyl-5-nitroimidazole) (Figure 1). Although the complex showed higher cytotoxic activity than the anticancer drug metronidazole itself,[20] further studies were not forthcoming. A series of compounds with the general formula [Ru(η^6-arene)Cl(en)][PF_6] (en = ethylenediamine; arene = benzene, *p*-cymene, tetrahydroanthracene, etc.) have been studied for their in vitro anticancer activity; e.g., one of the most active complexes, [Ru-(η^6-*p*-cymene)Cl(en)][PF_6] **5** (Figure 1), exhibits an IC_{50} value of 8 μM against the A2780 human ovarian cancer cell line.[21] In the same paper [Ru(η^6-*p*-cymene)Cl_2(isonicotinamide)] was described but found to be much less active than the ethylenediamine complexes.

Our research has focused on compounds of general formula [Ru(η^6-arene)Cl_2(pta)] (pta = 1,3,5-triaza-7-phosphaadamantane) (RAPTA), the prototype being [Ru(η^6-*p*-cymene)Cl_2(pta)] **6** (RAPTA-C) (Figure 1).[3,22] In vitro it exhibits pH-dependent DNA-damaging properties such that at pH < 7, which can be found in the tumor mass of poorly oxygenated cancer cells, DNA is damaged, whereas normal cells with pH > 7 are not

* To whom correspondence should be addressed. Phone: +41 (0)21 693 98 54. Fax: +41 (0)21 693 98 85. E-mail: paul.dyson@epfl.ch.
† Ecole Polytechnique Fédérale de Lausanne (EPFL).
‡ Callerio Foundation Onlus.
§ Università di Trieste.

[a] Abbreviations: en, ethylenediamine; ind, indazole; pta, 1,3,5-triaza-7-phosphaadamantane; imid, imidazole; mimid, *N*-methylimidazole; benzimid, benzimidazole; bimid, *N*-butylimidazole; vinylimid, *N*-vinylimidazole; benzoylimid, *N*-benzoylimidazole; [9]aneS_3, 1,4,7-trithiacyclononane; EE, ethyl acetate.

10.1021/jm060495o CCC: $33.50
Published on Web 08/09/2006

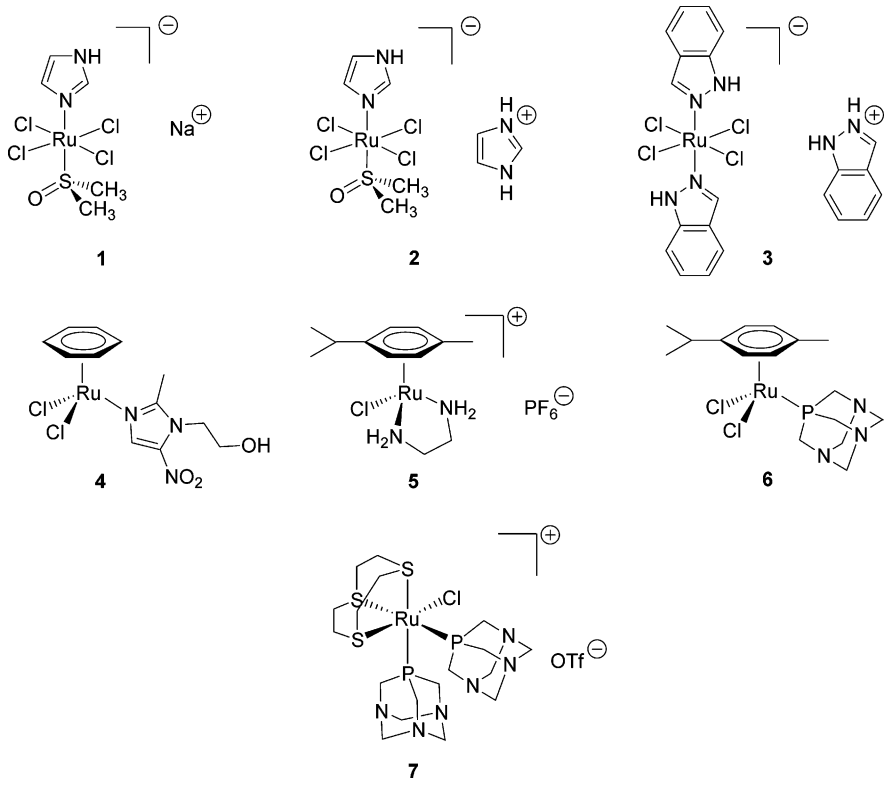

Figure 1. Structures of NAMI **1**, NAMI-A **2**, KP1019 **3**, [Ru(η^6-benzene)Cl_2(metronidazole)] **4**, [Ru(η^6-*p*-cymene)Cl(en)][PF_6] **5**, RAPTA-C **6**, and [RuCl(pta)$_2$([9]aneS_3)][OTf] **7**.

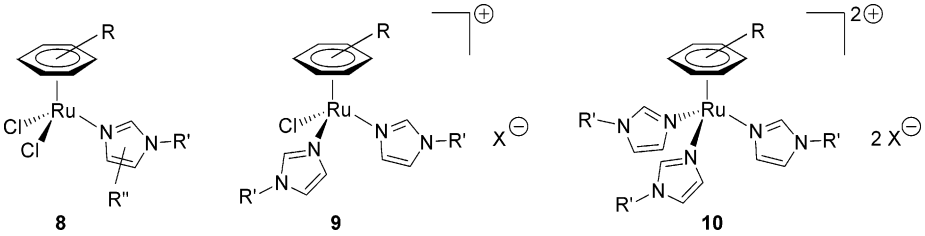

Figure 2. General structure of compounds **8**−**10**.

affected. Indeed, this selectivity was observed in comparative cell tests of several structural diversified RAPTA derivatives with TS/A adenocarcinoma cancer cells and nontumorigenic (healthy) HBL-100 mammary cells.[23] In vivo, **6** reduced significantly the growth of lung metastases in CBA mice bearing the MCa mammary carcinoma. Mass spectroscopic investigations revealed the lability of the arene moiety in RAPTA complexes during binding experiments with an oligonucleotide in cell-free medium.[24,25] Recent results indicate that the η^6-coordinated arene moiety in RAPTA-type compounds can be substituted by chelating ligands with three coordination sites such as 1,4,7-trithiacyclononane ([9]aneS_3), and in comparative cell studies, the complex [RuCl(pta)$_2$([9]aneS_3)][OTf] **7** (Figure 1) showed similar cytotoxicity and selectivity as **6**.[26]

In an attempt to synergistically combine the classes of substances, i.e., the Ru(II) piano-stool complexes such as **6**, with the imidazole ligand characteristic of NAMI-type ruthenium(III) complex, to obtain new potent anticancer drugs, in this study we describe the synthesis, crystallographic analysis, and preliminary in vitro biological evaluation of three new classes of Ru(II)-η^6-areneimidazole complexes **8**−**10** (Figure 2). Complexes of type [Ru(η^6-arene)Cl_2(ligand)] **8**, with one imidazole ligand, have already been reported,[27,28] including the monoimidazole derivative [Ru(η^6-C_6Me_6)Cl_2(imidazole)].[27] However, to the best of our knowledge, none of the existing examples have been evaluated for their anticancer properties. As far as we are aware, the bis-imidazole complexes of type [Ru(η^6-arene)Cl(ligand)$_2$][X] **9** and the tris-imidazole complexes of type [Ru(η^6-arene)(ligand)$_3$][X]$_2$ **10** are unprecidented, and a comparison of the in vitro activity of **8**−**10** should provide useful information for further biological evaluation and future drug design strategies.

Results and Discussion

The monoimidazole type complexes **8**, the pyridine analogue **11**, and the morpholine derivative **12** were prepared according to a protocol described by Bennett and Smith.[29] Treatment of [Ru(η^6-*p*-cymene)Cl_2]$_2$ with the corresponding stoichiometric amount, or a slight excess, of the amine in toluene under reflux for 2−3 h led to the complexes in reasonable to good yields (Figure 3). The desired compounds precipitated directly from the reaction mixture and were isolated by filtration. For the more labile ligand *N*-benzoylimidazole (benzoylimid), which was synthesized by a literature protocol,[30] the conversion was carried out in CH_2Cl_2 at room temperature.

In contrast to the other reactions, reaction with *N*-butylimidazole (bimid) did not lead to the formation of a precipitate. Therefore, an excess of petroleum ether was added, and the mixture was stored at 4 °C. After 6 weeks, large red crystals formed, which were identified by X-ray analysis as the ionic species [Ru(η^6-*p*-cymene)Cl(bimid)$_2$][Ru(η^6-*p*-cymene)Cl_3] **13** (Figure 3; also see the crystallographic section). To our

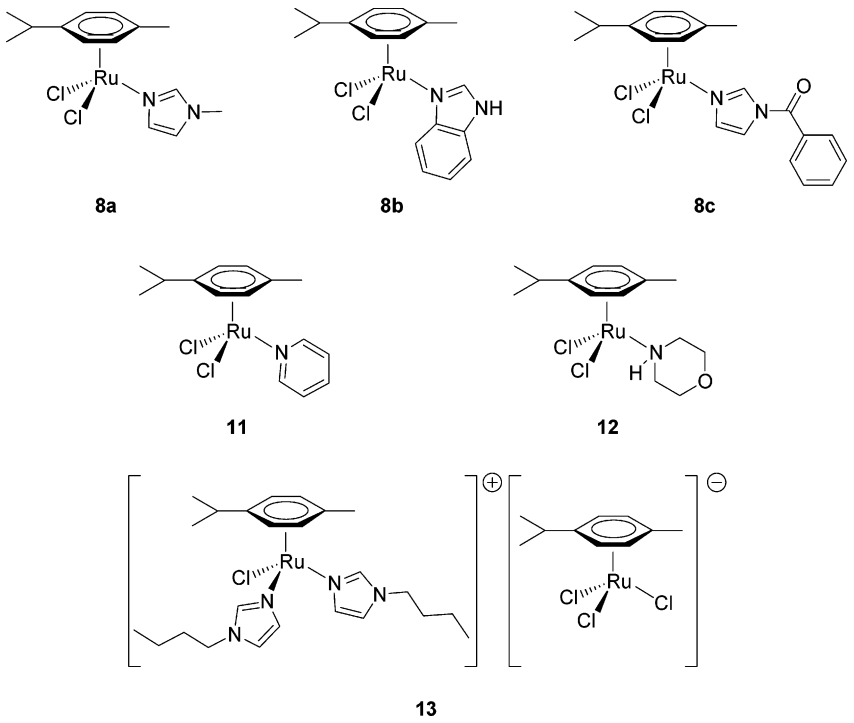

Figure 3. Structures of **8a**−**c** and **11**−**13**.

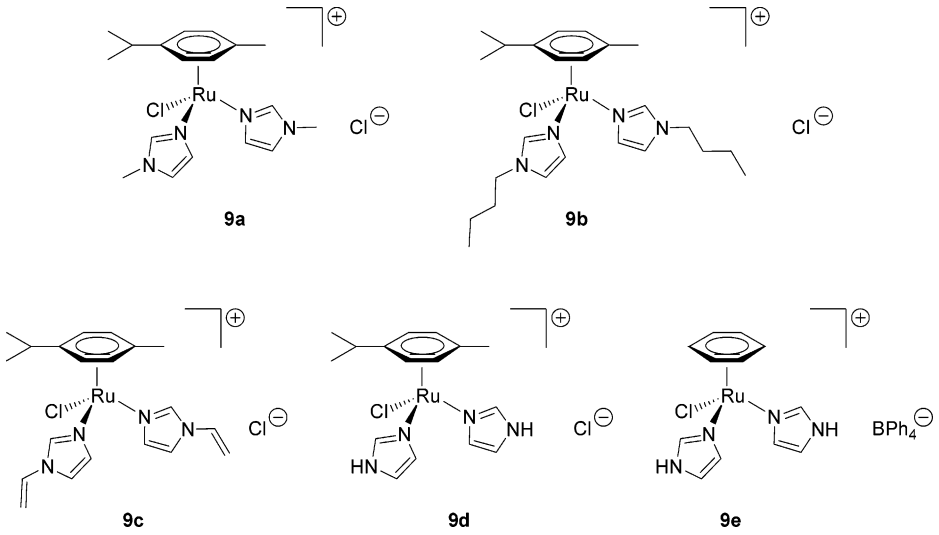

Figure 4. Structures of **9a**−**e**.

knowledge, the anion [Ru(η^6-*p*-cymene)Cl_3]$^-$ has only been reported once before[31] and a related trichlororuthenate(II) anion has also been prepared with different η^6-arene ligands,[32,33] but in each case synthesis was carried out in the presence of hydrochloric acid. In contrast, the formation of the ionic compound **13** proceeded under nonacidic conditions in a nonpolar solvent.

The synthesis of the bis-imidazole compounds, **9**, was generally performed by heating a mixture of the ruthenium precursor and 4 equiv of the appropiate ligand in a high-boiling alcoholic solvent such as *i*PrOH or *n*BuOH for 4−8 h (Figure 4), with the exception of [Ru(η^6-*p*-cymene)Cl(imid)$_2$][BPh_4] **9e** that was prepared in acetone in the presence of a slight excess of $NaBPh_4$. Use of an excess ligand led to slightly higher yields without the formation of higher substituted compounds, i.e., of type **10**. With the exception of **9a** the obtained yields were only moderate. Attempts to crystallize **9c**,**d** failed, and the solvent-wet compounds liquidified quickly with an accompanying color change to dark-brown when exposed to air, which might be due to their high hygroscopicity. However, thoroughly dried, the substances can be handled without problems. In general, the high hygroscopicity of the chloride salts **9a**−**d** is correlated with very high water solubility, which makes them ideal for physiological applications in terms of administration.

Compounds **10** (Figure 5) were prepared by treatment of the corresponding ruthenium(II) precursor with a slight excess of *N*-methylimidazole and $AgBF_4$ in CH_2Cl_2 or $CHCl_3$ under ambient conditions, leading to compounds **10a** and **10b** in modest yield. The substances exhibited good to very good water solubility.

The ESI mass spectra of **8**−**10** in methanol or CH_3CN provide parent peaks corresponding to the cations for **9** and **10**, and in the case of **8** loss of one chloride ligand takes place to generate a cation. For compounds **8** and **9**, varying degrees of solvated species are also observed; nonetheless, all spectra confirm the presence of the expected products.

The assignment of the imidazole ^1H and ^{13}C NMR signals in the series of homologous complexes [Ru(η^6-*p*-cymene)Cl_2-

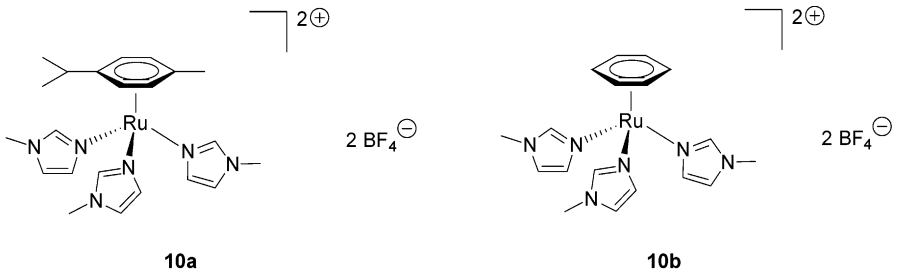

Figure 5. Structures of complexes **10a,b**.

Table 1. Selected Bond Lengths (in Å) and Angles (deg) for Complexes **9a**, **9b**, **9e**, **10b**, and **13**

parameter	**9a** (Ar = *p*-cymene; R = Me)	**9b** (Ar = *p*-cymene; R = *n*Bu)	**13** (cation) (Ar = *p*-cymene; R = *n*Bu)	**9e** (Ar = benzene; R = H)	**10b** (Ar = benzene; R = Me)
Ru−N(imid(R))	2.121(3)	2.122(2)	2.110(5)	2.114(3)	2.107(2)
	2.131(3)	2.123(2)	2.131(5)	2.122(3)	2.108(2)
					2.110(2)
Ru−Cl	2.432(5)	2.422(1)	2.415(2)	2.407(1)	
Ru−$Ar_{centriod}$	1.684	1.668	1.669	1.671	1.678
N(imid(R))−Ru−N(imid(R))	83.02(6)	84.56(12)	85.87(18)	85.00(13)	82.07(6)
					85.53(6)
					90.37(6)
Cl−Ru−N(imid(R))	86.61(5)	87.47(9)	87.57(13)	86.44(9)	
	87.44(5)	88.19(10)	87.77(13)	85.61(9)	
$Ar_{centriod}$−Ru−N(imid(R))	128.88	127.67	127.12	128.88	125.41
	129.98	128.41	128.43	129.23	127.71
					131.15
$Ar_{centriod}$−Ru−Cl	125.99	126.55	126.38	126.67	

(mimid)] **8a**, [Ru(η^6-*p*-cymene)Cl(mimid)$_2$][Cl] **9a**, and [Ru(η^6-*p*-cymene)(mimid)$_3$][BF_4]$_2$ **10a** was based on 2D NMR experiments in combination with spectroscopic data and calculations of Standfest-Hauser et al.[34] and Caballero et al.,[35] dealing with related complexes. For the ^{13}C NMR data, only minor changes are observed between the complexes. However, it must be mentioned that the NMR spectra of **10a** were measured in acetone-d_6 instead of $CDCl_3$, which only allows a tentative comparison between the spectral data sets. A continuous shift to higher frequencies of $\Delta\delta = 3.1$ ppm is observed for the resonance of C-2′ as the number of imidazole ligands at the ruthenium(II) center increases. For C-4′ and C-5′, no such trend is observed. In comparison, very strong changes are observed for the ^{1}H NMR resonances of the imidazole protons. Between complexes **8a** and **9a**, the signals of 2′-H and 5′-H are shifted to higher frequencies with $\Delta\delta = 1.32$ ppm and $\Delta\delta = 0.29$ ppm, respectively. The frequencies for **10a** are similar to **8a** and not, as perhaps could be expected, to **9a**. For 4′-H, a continuous but only small shift to lower frequencies of $\Delta\delta = 0.17$ ppm is observed when changing from **8a** to **10a**. The proton in the 2′-position becomes more acidic when two imidazole ligands are attached to the ruthenium center, and to a lesser extent this trend is also valid for 5′-H. The most extreme position of a signal corresponding to 2′-H is detected at 9.73 ppm for the complex [Ru(η^6-*p*-cymene)Cl(vinylimid)$_2$][Cl] **9c**. The resonances of 2′-H for the N-unsubstituted imidazoles **8b**, **9d**, and **9e** are found at 8.03−8.28 ppm. The corresponding peak for **8c** is detected at 8.51 ppm.

Characterization of the Complexes 9a, 9b, 9e, 10b, and 13 by X-ray Diffraction. For a set of representative complexes, single crystals suitable for crystallographic structure analysis by X-ray diffraction were obtained.[36] All structures display the ubiquitous three-legged piano-stool geometry; important bond lengths and angles are listed in Table 1. Complex **9a** (Figure 6) was found to crystallize with two cations, two chloride anions, and two water solvates (with the oxygen centers facing one another) per unit cell. The *p*-cymene group of the metal cation is rotated to eclipse one of the imidazole ligands with the methyl substituent. Conversely, the bulkier isopropyl substituent points away from the imidazole and chloride ligands. The facial orientation of the imidazole ligands in the solid state is determined primarily by intermolecular interactions. This is verified by an analysis of the packing structure, which shows that the hydrogen atoms of one *N*-methylimidazole ligand exhibit intermolecular interactions with the chloride anions and a single oxygen of water and vice versa for the second imidazole group. The *p*-cymene group also forms some weak interactions with the anionic moieties.

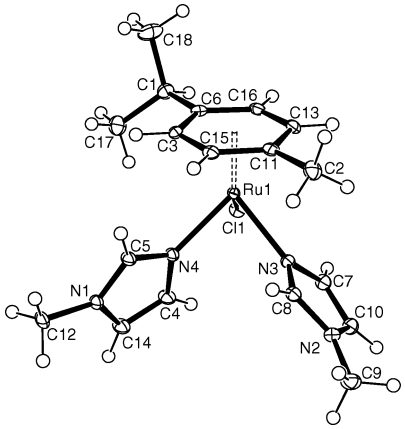

Figure 6. ORTEP figure of **9a** drawn with 30% probability ellipsoids. Anion and water solvate have been omitted for clarity.

When the imidazole groups are fitted with a longer alkyl chain (i.e., *n*-butyl), a different spatial orientation of the ligands is obtained (Figure 7). Two different complexes containing the cation [Ru(η^6-*p*-cymene)Cl(bimid)$_2$]$^+$ were crystallographically studied, one with a simple Cl^- counterion (**9b**, Figure 7) and another one with the very rarely seen monomeric anion [Ru(η^6-*p*-cymene)Cl_3]$^-$ (**13**, Figure 8), reported only once previ-

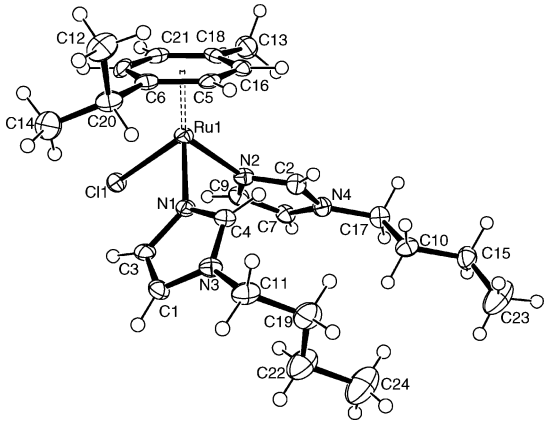

Figure 7. ORTEP figure of **9b** drawn with 30% probability ellipsoids. The anion has been omitted for clarity.

ously.[31] In both cases, the alkyl substituents of the *p*-cymene moiety eclipse both bimid ligands. The Ru−Cl and Ru−N bond distances for **9b** (2.422(1), 2.123(3), 2.121(3) Å) and **13** (2.415(2), 2.110(5), 2.131(5) Å) remain identical within experimental error to those in **9a** (2.432(1), 2.121(2), 2.131(2) Å). However, the N−Ru−N angle increases slightly from 83.02(6)° in **9a** to 84.56(12)° in **9b** and 85.53(6)° in **13**. The longer aliphatic chain has the effect of reducing the number of intermolecular associations. The majority of present interactions are centered around the bound chloride groups of the anion and the *p*-cymene ligand. However, for **13**, one imidazole group is tilted slightly more to form a weak interaction with the anion. In **9b**, the hydrogens (H2A and H4A) form a symmetric bifurcating interaction with the chloride (H2A···Cl1 2.520 Å, H4A···Cl1 2.586 Å).

The remaining two compounds that were investigated feature a η^6-coordinated benzene instead of *p*-cymene. For **9e** (Figure 9), the first attempt to solve the structure yielded a mixture of the cations $[Ru(\eta^6\text{-benzene})Cl(imid)_2]^+$ and $[Ru(\eta^6\text{-benzene})(OH)(imid)_2]^+$ in a 9:1 ratio. Regrowing the crystals under more anhydrous conditions yielded a structure containing only the chloride containing species. Interestingly, the N−H protons for both imidazole ligands are engaged in a π-type interaction with a phenyl group of the borate anion. An extended structure is thus formed between alternating imidazole groups of the cation and phenyls of the anion. This type of interaction is uncommon, but it has been observed in the free N-protonated and N-methylated imidazolium salts containing BPh_4^-.[37] The Ru−Cl distance is slightly shorter (2.407(1) Å) than for the corresponding *p*-cymene analogues, with the Ru−N bonds (2.122(3) and 2.114(3) Å) being equivalent as well as the N−Ru−N bond angle (85.00(13)°). Another difference between the η^6-*p*-cymene and η^6-benzene coordinated structures is the orientation of the imidazole ligand, where in the former, the (Ru)N−C(H)−N(R) component is always pointing toward the arene and the (Ru)N−C(H)−C(H)−N(R) part is directed toward the Cl ligand. However, in the benzene structure **9e** (Ar = C_6H_6, R = H), the ligands are rotated 180° with respect to one another to allow for the π-type interaction with the phenyl groups of the borate anion.

Representative for η^6-arene ruthenium(II) trisimidazole complexes of type **10**, a crystal structure was collected for **10b** (Figure 10). The Ru−N bond distances (2.107(2), 2.108(2), 2.111(2) Å) are equivalent to those for complexes of type **8** and **9**. In **10b**, the imidazole ligands are arranged into a quasi-C_3 symmetric propeller conformation around the Ru−benzene axis. The two BF_4^- anions lie almost parallel to the arene ring, fitted into the pocket defined by two imidazole ligands. In general, the doubly cationic nature of the complex results in closer anion interactions compared to the other complexes.

Cell Growth Inhibition Effects on TS/A Adenocarcinoma Cells and HBL-100 Mammary Cells. The biological MTT (3-(4,5-dimethylthiazol-2-yl)-2,5-diphenyltetrazolium bromide) test, which measures mitochondrial dehydrogenase activity as an indication of cell viability, was carried out with all these water-soluble compounds except for complex **9e** because of its very low solubility in water. The experiments were performed on two different cell lines, tumor mouse TS/A cells and normal human HBL-100 cells, a comparison of cytotoxicity between the cell lines (the latter as a model for healthy cells) being used to identify RAPTA compounds as selective antitumor agents.[23,25] The effects of these ruthenium compounds on the cell growth were evaluated by measuring the variations after treatment for 24, 48, and 72 h. The IC_{50} values for all the compounds studied are listed in Table 2 for both cell lines (see Supporting Information, Figure S1, for graphs of the cytotoxic effects).

Compared to cisplatin, for example, from Table 2 it is clear that all the ruthenium areneimidazole complexes are far less cytotoxic, yet their cytotoxicities are not too dissimilar to other ruthenium complexes such as **6** and its toluene derivative [Ru(η^6-toluene)Cl_2(pta)] (RAPTA-T) (see Table 2).[23,25] Type **8** compounds exert very little differences in cytotoxicity between the two cell lines, taken as an indication of potentially poor selectivity in vivo.

Compounds **9a** and **9d** do not show any toxicity toward either cell line even at 1000 μM concentrations. The two compounds, which contain pyridine and morpholine (as opposed to imidazoles), are the only compounds that are actually more cytotoxic toward the model healthy cells (HBL-100) compared to the cancer cell model. Combined, it is interesting to note that the ruthenium complexes that have reached clinical trials to date are endowed with imidazole or indazole ligands and not other amines, although their precise roles remain unknown.[9,38]

The remaining complexes, **9b**, **9c**, **10a**, and **10b**, are all more cytotoxic in the TS/A cancer cell line than the healthy cell model, the most cytotoxic being **10a** but the one showing the greatest difference in cytotoxicity being [Ru(η^6-*p*-cymene)Cl(vinylimid)$_2$][Cl] **9c**, which is 2.7-fold more cytotoxic toward the cancer cells, and $[Ru(\eta^6\text{-benzene})(mimid)_3][BF_4]_2$ **10b**, which is 3-fold more cytotoxic. Such selective cytotoxicity is characteristic not only of the RAPTA compounds but also of the [9]aneS_3 analogues (e.g., **7** in Figure 1) with pta and ethylenediamine as coligands.[26] Although the cationic ruthenium(II) arene ethylenediamine complexes introduced by Sadler et al.[21,39,40] (e.g., **5** Figure 1) display significantly higher cytotoxicities in A2780 human ovarian cancer cells, at best IC_{50} = 2 μM for [RuCl(η^6-dihydroanthracene)(en)][PF_6], which is similar to the value of cisplatin with IC_{50} = 0.5 μM,[40] a direct comparison is difficult, since these compounds have not been evaluated against the same cancer cell/healthy cell model for the determination of selectivity. As far as we are aware, the ruthenium(II) arene imidazole derivatives **9c** and **10b** represent the first compounds of this general type without the pta ligand to exert such a selectivity in the in vitro assay. While both these compounds have been selected for further studies, these data indicate that it is still too early to discern a parallel between compound structure and biological response, especially since the most selective compounds were those with substituted imidazoles rather than imidazole itself that is present in NAMI-A.

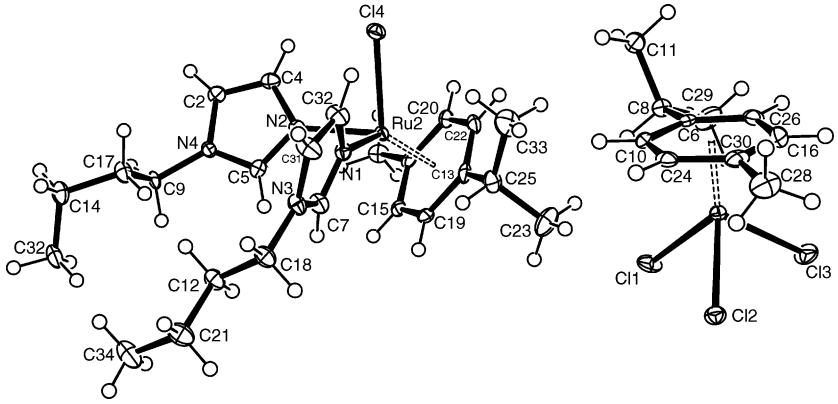

Figure 8. ORTEP plot of **13** drawn with 30% probability ellipsoids.

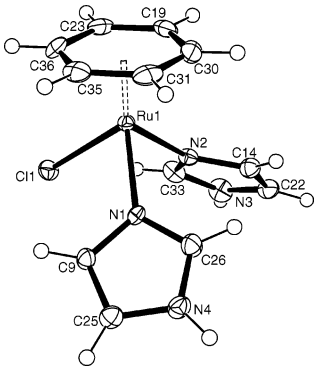

Figure 9. ORTEP figure of **9e** drawn with 30% probability ellipsoids. The anion has been omitted for clarity.

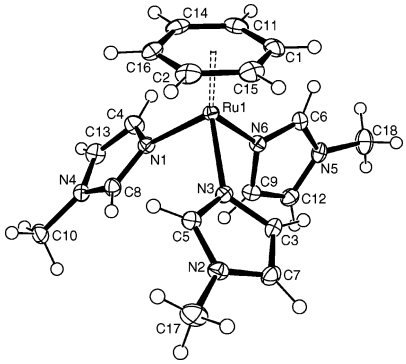

Figure 10. ORTEP figure of **10b** drawn with 30% probability ellipsoids. The anion has been omitted for clarity.

Experimental Details

Synthesis and Chemical Characterization. $[RuCl_2(\eta^6\text{-}p\text{-cymene})]_2$ and $[RuCl_2(\eta^6\text{-benzene})]_2$ were synthesized following a literature protocol.[41] All other reagents and solvents were obtained from commercial sources and used without further purification. ^1H and ^{13}C NMR spectra were recorded on a Bruker 400 MHz spectrometer at room temperature in $CDCl_3$, acetone-d_6, DMSO-d_6 or MeOH-d_4. The NMR spectra were referenced to internal solvents as follows: δ ($CHCl_3$, ^1H) = 7.26 and δ ($CDCl_3$, ^{13}C) = 77.00; δ (acetone-d_5, ^1H) = 2.05 and δ (acetone-d_6, ^{13}C) = 29.84; δ (DMSO-d_5, ^1H) = 2.50 and δ (DMSO-d_6, ^{13}C) = 39.52; δ (MeOH-d_3, ^1H) = 3.31 and δ (MeOH-d_4, ^{13}C) = 49.00.[42] Structures showing the numbering scheme for the NMR assignments are provided in Supporting Information. Electrospray ionization mass spectra (ESI-MS) were recorded on a Thermofinigan LCQ Deca XP Plus quadrupole ion trap instrument in positive mode in MeOH or CH_3CN following a literature procedure.[43] Elemental analyses were provided by the analytical services of EPFL.

[Ru(η^6-*p*-cymene)Cl_2(pyridine)] (11). To a suspension of [Ru(η^6-*p*-cymene)Cl_2]$_2$ (100 mg, 0.163 mmol) in toluene (15 mL), pyridine (30 μL, 0.37 mmol, 2.3 equiv) was added at room temperature. The resulting mixture was heated to reflux for 3 h. After the mixture was cooled, the precipitate was filtered, washed with petroleum ether (3 × 10 mL), and dried in vacuo, affording an orange microcristalline solid (78.7 mg, 0.204 mmol, 63%). ^1H NMR (400 MHz, $CDCl_3$): δ = 1.31 (d, J = 6.9 Hz, 6 H, 1-CH(CH_3)$_2$), 2.10 (s, 3 H, 4-CH_3), 3.00 (sept, J = 6.9 Hz, 1 H, 1-CH(CH_3)$_2$), 5.22 (d, J = 6.0 Hz, 2 H, 2-H, 6-H), 5.44 (d, J = 6.0 Hz, 2 H, 3-H, 5-H), 7.31 (ddd (strongly irregular), J = 7.6, 5.2, 1.4 Hz, 2 H, 3′-H, 5′-H), 7.74 (tt, J = 7.6, 1.4 Hz, 1 H, 4′-H), 9.05 (dt (strongly irregular), J = 5.2, 1.4 Hz, 2 H, 2′-H, 6′-H). ^{13}C NMR (100 MHz, $CDCl_3$): δ = 18.18 (4-CH_3), 22.27 (1-CH(CH_3)$_2$), 30.63 (1-CH(CH_3)$_2$), 82.23 (C-2, C-6), 82.77 (C-3, C-5), 97.02 (C-4), 103.5 (C-1), 124.5 (C-3′, C-5′), 137.5 (C-4′), 154.9 (C-2′, C-6′). ESI-MS (CH_3CN): m/z (%) = 390.4 (21) [Ru(cymene)Cl(CH_3CN)(pyridine)]$^+$, 349.9 (49) [Ru(cymene)Cl(pyridine)]$^+$, 311.9 (100) [Ru(cymene)Cl(CH_3CN)]$^+$.

Table 2. IC_{50} Values of the Complexes on TS/A and HBL-100 Cell Lines after 72 h of Incubation

compd	IC_{50} (μM) TS/A	IC_{50} (μM) HBL-100
[Ru(η^6-*p*-cymene)Cl_2(pyridine)] (**11**)	757	522
[Ru(η^6-*p*-cymene)Cl_2(morpholine)] (**12**)	640	523
[Ru(η^6-*p*-cymene)Cl_2(mimid)] (**8a**)	659	790
[Ru(η^6-*p*-cymene)Cl_2(benzimid)] (**8b**)	573	601
[Ru(η^6-*p*-cymene)Cl_2(benzoylimid)] (**8c**)	723	895
[Ru(η^6-*p*-cymene)Cl(mimid)$_2$][Cl]·H_2O (**9a**)	>1000	>1000
[Ru(η^6-*p*-cymene)Cl(bimid)$_2$][Cl] (**9b**)	172	238
[Ru(η^6-*p*-cymene)Cl(vinylimid)$_2$][Cl] (**9c**)	361	990
[Ru(η^6-*p*-cymene)Cl(imid)$_2$][Cl] (**9d**)	>1000	>1000
[Ru(η^6-*p*-cymene)(mimid)$_3$][BF_4]$_2$ (**10a**)	136	172
[Ru(η^6-benzene)(mimid)$_3$][BF_4]$_2$ (**10b**)	249	740
[Ru(η^6-*p*-cymene)Cl_2(pta)] (**6**)[23]	>300	>300
[Ru(η^6-toluene)Cl_2(pta)][23]	74	>300

[Ru(η^6-*p*-cymene)Cl_2(morpholine)] (12). To a suspension of [Ru(η^6-*p*-cymene)Cl_2]$_2$ (100 mg, 0.163 mmol) in toluene (15 mL), morpholine (30 μL, 0.34 mmol, 2.1 equiv) was added at room temperature. The resulting mixture was heated to reflux for 3 h. After the mixture was cooled, the precipitate was filtered, washed with petroleum ether (4 × 10 mL), and dried in vacuo, affording an orange microcristalline solid (96.0 mg, 0.244 mmol, 75%). ^1H NMR (400 MHz, $CDCl_3$): δ = 1.30 (d, J = 6.9 Hz, 6 H, 1-CH(CH_3)$_2$), 2.23 (s, 3 H, 4-CH_3), 2.42 (br m_c, 1 H, NH), 3.02 (sept, J = 6.9 Hz, 1 H, 1-CH(CH_3)$_2$), 3.23 (qd, J = 12.4 Hz, J_{AB} = 3.1 Hz, 2 H, 2′-H_A, 6′-H_A), 3.45 (td, J = 12.4 Hz, J_{AB} = 1.6 Hz, 2 H, 3′-H_A, 5′-H_A), 3.65 (br d, J = 12.4 Hz, 2 H, 3′-H_B, 5′-H_B), 3.86 (dd, J = 12.4 Hz, J_{AB} = 3.1 Hz, 2 H, 2′-H_B, 6′-H_B), 5.30 (d, J = 6.1 Hz, 2 H, 2-H, 6-H), 5.34 (d, J = 6.1 Hz, 2 H, 3-H, 5-H). ^{13}C NMR (100 MHz, $CDCl_3$): δ = 18.39 (4-CH_3), 21.98 (1-CH(CH_3)$_2$), 30.92 (1-CH(CH_3)$_2$), 54.10 (C-2′, C-6′), 69.09 (C-3′, C-5′), 78.00 (C-2, C-6), 82.93 (C-3, C-5), 93.36 (C-4), 104.9 (C-1). ESI-MS (CH_3CN): m/z (%) = 494.6 (29) [Ru(cymene)(morpholine)$_3$ − H]$^+$,

398.6 (100) [Ru(cymene)Cl(CH_3CN)(morpholine)]$^+$, 352.6 (12) [Ru(cymene)Cl(CH_3CN)$_2$]$^+$.

[Ru(η^6-*p*-cymene)Cl$_2$(mimid)] (8a). To a suspension of [Ru(η^6-*p*-cymene)Cl$_2$]$_2$ (100 mg, 0.163 mmol) in toluene (15 mL), *N*-methylimidazole (26 μL, 0.33 mmol, 2.0 equiv) was added at room temperature. The resulting mixture was heated to reflux for 3 h. After the mixture was cooled, the precipitate was filtered, washed with petroleum ether (4 × 10 mL), and dried in vacuo, affording a brown, slightly sticky, and hygroscopic solid (58.7 mg, 0.151 mmol, 46%). ^{1}H NMR (400 MHz, $CDCl_3$): δ = 1.28 (d, J = 6.9 Hz, 6 H, 1-CH(CH_3)$_2$), 2.19 (s, 3 H, 4-CH_3), 2.99 (sept, J = 6.9 Hz, 1 H, 1-CH(CH$_3$)$_2$), 3.65 (s, 3 H, 1″-H$_3$), 5.25 (d, J = 5.7 Hz, 2 H, 2-H, 6-H), 5.44 (d, J = 5.7 Hz, 2 H, 3-H, 5-H), 6.85 (br s, 1 H, 4′-H), 7.30 (br s, 1 H, 5′-H), 7.87 (br s, 1 H, 2′-H). ^{13}C NMR (100 MHz, $CDCl_3$): δ = 18.54 (4-*C*H$_3$), 22.22 (1-CH(*C*H$_3$)$_2$), 30.65 (1-*C*H(CH$_3$)$_2$), 34.52 (C-1″), 81.41 (C-2, C-6), 82.45 (C-3, C-5), 97.24 (C-4), 102.6 (C-1), 120.7 (C-4′), 132.2 (C-5′), 140.4 (C-2′). ESI-MS (CH_3CN): *m*/*z* (%) = 393.4 (10) [Ru(cymene)Cl(CH_3CN)(mimid)]$^+$, 353.0 (100) [Ru(cymene)Cl(mimid)]$^+$, 311.9 (28) [Ru(cymene)Cl(CH_3CN)]$^+$.

[Ru(η^6-*p*-cymene)Cl$_2$(benzimid)] (8b). To a suspension of [Ru(η^6-*p*-cymene)Cl$_2$]$_2$ (100 mg, 0.163 mmol) in toluene (15 mL), benzimidazole (40.0 mg, 0.339 mmol, 2.08 equiv) was added at room temperature. The resulting mixture was heated to reflux for 2.5 h. After the mixture was cooled, the precipitate was filtered, washed with petroleum ether (4 × 10 mL), and dried in vacuo, affording an orange-brown solid (88.0 mg, 0.207 mmol, 64%). ^{1}H NMR (400 MHz, $CDCl_3$): δ = 1.26 (d, J = 6.9 Hz, 6 H, 1-CH(CH_3)$_2$), 2.04 (s, 3 H, 4-CH_3), 2.87 (sept, J = 6.9 Hz, 1 H, 1-CH(CH$_3$)$_2$), 5.39 (d, J = 5.7 Hz, 2 H, 2-H, 6-H), 5.57 (d, J = 5.7 Hz, 2 H, 3-H, 5-H), 6.60−6.66 (br m, 2 H, 6′-H, 7′-H), 6.92−7.00 (br m, 1 H, 5′-H), 7.60 (d, J = 8.2 Hz, 1 H, 4′-H), 8.12 (br s, 1 H, 2′-H), 10.44 (br s, 1 H, NH). ^{13}C NMR (100 MHz, $CDCl_3$): δ = 18.44 (4-*C*H$_3$), 22.24 (1-CH(*C*H$_3$)$_2$), 30.64 (1-*C*H(CH$_3$)$_2$), 80.78 (C-2, C-6), 82.73 (C-3, C-5), 97.32 (C-4), 102.6 (C-1), 112.5 (C-7′), 118.5 (C-4′), 121.9 (C-5′), 123.2 (C-6′), 132.1 (C-7′a), 140.0 (C-3′a), 144.7 (C-2′). ESI-MS (CH_3CN): *m*/*z* (%) = 429.5 (100) [Ru(cymene)Cl(CH_3CN)(benzimid)]$^+$, 389.0 (26) [Ru(cymene)Cl(benzimid)]$^+$, 352.5 (23) [Ru(cymene)Cl(CH_3CN)$_2$]$^+$, 311.9 (52) [Ru(cymene)Cl(CH_3CN)]$^+$.

Synthesis of *N*-Benzoylimidazole (Benzoylimid). To a solution of imidazole (1.36 g, 20 0 mmol, 2.00 equiv) in CH_2Cl_2 (15 mL), benzoyl chloride (1.16 mL, 9.99 mmol) was added at room temperature over 3 min. The resulting mixture was stirred at room temperature for 75 min. The precipitate was filtered and washed with CH_2Cl_2 (3 × 5 mL). The combined filtrates were evaporated in vacuo, affording a slightly yellow oily liquid that was used without further purification. ^{1}H NMR (400 MHz, $CDCl_3$): δ = 7.16−7.18 (br m, 1 H, 4-H), 7.52−7.59 (m, 3 H, 5-H, 3′-H, 5′-H), 7.69 (tt, J = 6.9, 1.5 Hz, 1 H, 4′-H), 7.80 (dt, J = 6.6, 1.5 Hz, 2′-H, 6′-H), 8.08 (br s, 1 H, 2-H).

[Ru(η^6-*p*-cymene)Cl$_2$(benzoylimid)] (8c). To a solution of [Ru(η^6-*p*-cymene)Cl$_2$]$_2$ (250 mg, 0.408 mmol) in CH_2Cl_2 (10 mL), a solution of *N*-benzoylimidazole (142 mg, 0.825 mmol, 2.02 equiv) in CH_2Cl_2 (3 mL) was added at room temperature. The resulting mixture was stirred at room temperature for 2 h. Addition of petroleum ether (60 mL) led to the separation of an oil, which was redissolved by addition of CH_2Cl_2 (50 mL). The solution was reduced in vacuo to a volume of approximately 20 mL. Strong crystallization set in, which was accomplished by keeping the solution at room temperature for an additional 30 min. The precipitate was filtered with suction, washed with petroleum ether (2 × 10 mL), and dried in vacuo, affording an orange-brown crystalline solid (320 mg, 0.669 mmol, 82%). ^{1}H NMR (400 MHz, $CDCl_3$): δ = 1.30 (d, J = 6.9 Hz, 6 H, 1-CH(CH_3)$_2$), 2.21 (s, 3 H, 4-CH_3), 2.99 (sept, J = 6.9 Hz, 1 H, 1-CH(CH$_3$)$_2$), 5.30 (d, J = 5.8 Hz, 2 H, 2-H, 6-H), 5.48 (d, J = 5.8 Hz, 2 H, 3-H, 5-H), 7.49 (s, 1 H, 5′-H), 7.55 (s, 1 H, 4′-H), 7.56 (t, J = 7.6 Hz, 2 H, 3″-H, 5″-H), 7.70 (t, J = 7.6 Hz, 1 H, 4″-H), 7.77 (d, J = 7.6 Hz, 2 H, 2″-H, 6″-H), 8.51 (s, 1 H, 2′-H). ^{13}C NMR (100 MHz, $CDCl_3$): δ = 18.61 (4-*C*H$_3$), 22.22 (1-CH(*C*H$_3$)$_2$), 30.72 (1-*C*H(CH$_3$)$_2$), 81.49 (C-2, C-6), 82.57 (C-3, C-5), 97.58 (C-4), 103.1 (C-1), 118.2 (C-5′), 129.3 (C-3″, C-5″), 130.1 (C-2″, C-6″), 133.0 (C-4′), 134.5 (C-4″), 141.7 (C-2′), 164.7 (N*C*O). ESI-MS (CH_3CN): *m*/*z* (%) = 483.4 (100) [Ru(cymene)Cl(CH_3CN)(benzoylimid)]$^+$, 443.0 (65) [Ru(cymene)Cl(benzoylimid)]$^+$, 352.5 (65) [Ru(cymene)Cl(CH$_3$-CN)$_2$]$^+$, 311.9 (67) [Ru(cymene)Cl(CH_3CN)]$^+$.

[Ru(η^6-*p*-cymene)Cl(mimid)$_2$][Cl]·H$_2$O (9a). To a suspension of [Ru(η^6-*p*-cymene)Cl$_2$]$_2$ (100 mg, 0.163 mmol) in *i*PrOH (15 mL), *N*-methylimidazole (100 μL, 1.26 mmol, 7.73 equiv) was added at room temperature. The resulting mixture was heated to reflux for 8 h. The solvent was removed in vacuo. The residue was taken up in CH_2Cl_2, and an excess of EE was added. CH_2Cl_2 was removed in vacuo. The obtained turbid solution was decanted from a precipitated slimy solid and kept standing in air at room temperature for several hours. Orange crystals precipitated, which were also suitable for X-ray analysis. The precipitate was filtered and dried in vacuo, affording an orange crystalline solid (117 mg, 0.240 mmol, 73%). ^{1}H NMR (400 MHz, $CDCl_3$): δ = 1.13 (d, J = 6.9 Hz, 6 H, 1-CH(CH_3)$_2$), 1.78 (s, 3 H, 4-CH_3), 2.37 (sept, J = 6.9 Hz, 1 H, 1-CH(CH$_3$)$_2$), 3.77 (s, 6 H, 2 × 1″-H$_3$), 5.83 (d, J = 6.3 Hz, 2 H, 2-H, 6-H), 5.86 (d, J = 6.3 Hz, 2 H, 3-H, 5-H), 6.77 (t, J = 1.5 Hz, 2 H, 2 × 4′-H), 7.59 (t, J = 1.5 Hz, 2 H, 2 × 5′-H), 9.19 (br s, 2 H, 2 × 2′-H). ^{13}C NMR (100 MHz, $CDCl_3$): δ = 17.85 (4-*C*H$_3$), 22.21 (1-CH(*C*H$_3$)$_2$), 30.73 (1-*C*H(CH$_3$)$_2$), 34.69 (2 × C-1″), 82.19 (C-2, C-6), 85.92 (C-3, C-5), 100.4 (C-4), 103.3 (C-1), 120.6 (2 × C-4′), 130.6 (2 × C-5′), 142.1 (2 × C-2′). ESI-MS (MeOH): *m*/*z* (%) = 565.1 (5) [Ru$_2$(cymene)$_2$(MeOH)$_3$]$^+$, 434.9 (100) [Ru(cymene)(mimid)$_2$Cl]$^+$, 353.1 (4) [Ru(cymene)(mimid)Cl]$^+$.

[Ru(η^6-*p*-cymene)Cl(bimid)$_2$][Cl] (9b). To a suspension of [Ru(η^6-*p*-cymene)Cl$_2$]$_2$ (100 mg, 0.163 mmol) in *i*PrOH (15 mL), *N*-butylimidazole (150 μL, 1.14 mmol, 7.00 equiv) was added at room temperature. The resulting mixture was heated to reflux for 8 h. The solvent was evaporated in vacuo. The residue was taken up in EE, and the solution was filtered over a short pad of silica gel. Excess of imidazole ligand was washed down with EE, and the ruthenium complex was subsequently eluted with $CHCl_3$/EtOH (3:1). Evaporation of the solvent and crystallization of the residue from EE/Et$_2$O yielded a yellow crystalline compound (91.1 mg, 0.164 mmol, 50%). Crystals suitable for X-ray analysis were obtained by slow crystallization from EE/Et$_2$O. ^{1}H NMR (400 MHz, $CDCl_3$): δ = 0.90 (t, J = 7.4 Hz, 6 H, 2 × 4″-H$_3$), 1.12 (d, J = 6.9 Hz, 6 H, 1-CH(CH_3)$_2$), 1.16−1.32 (m, 4 H, 2 × 3″-H$_2$), 1.71−1.79 (m, 4 H, 2 × 2″-H$_2$), 1.77 (s, 3 H, 4-CH_3), 2.37 (sept, J = 6.9 Hz, 1 H, 1-CH(CH$_3$)$_2$), 4.01 (t, J = 7.2 Hz, 4 H, 2 × 1″-H$_2$), 5.85 (d, J = 6.1 Hz, 2 H, 2-H, 6-H), 5.89 (d, J = 6.1 Hz, 2 H, 3-H, 5-H), 6.79 (t, J = 1.4 Hz, 2 H, 2 × 4′-H), 7.62 (t, J = 1.4 Hz, 2 H, 2 × 5′-H), 9.22 (t, J = 1.4 Hz, 2 H, 2 × 2′-H). ^{13}C NMR (100 MHz, $CDCl_3$): δ = 13.46 (2 × C-4″), 17.80 (4-*C*H$_3$), 19.47 (2 × C-3″), 22.22 (1-CH(*C*H$_3$)$_2$), 30.81 (1-*C*H(CH$_3$)$_2$), 32.58 (2 × C-2″), 47.92 (2 × C-1″), 82.32 (C-2, C-6), 85.94 (C-3, C-5), 100.4 (C-4), 103.3 (C-1), 119.1 (2 × C-4′), 130.5 (2 × C-5′), 141.5 (2 × C-2′). ESI-MS (MeOH): *m*/*z* (%) = 519.0 (100) [Ru(cymene)-(bimid)$_2$Cl]$^+$, 395.3 (6) [Ru(cymene)(bimid)Cl]$^+$.

[Ru(η^6-*p*-cymene)Cl(vinylimid)$_2$][Cl] (9c). To a suspension of [Ru(η^6-*p*-cymene)Cl$_2$]$_2$ (100 mg, 0.163 mmol) in *n*BuOH (15 mL), *N*-vinylimidazole (60 μL, 0.66 mmol, 4.0 equiv) was added at room temperature. The resulting mixture was heated to reflux for 4 h. The solvent was removed in vacuo as azeotrope with toluene. The residue was taken up in CH_2Cl_2, and an excess of EE was added. CH_2Cl_2 was removed in vacuo. Addition of a large excess of Et$_2$O led to the formation of a yellow precipitate. The supernatant was pipetted off. The precipitate was washed with Et$_2$O (2 × 5 mL) and dried in vacuo, affording a yellow, very moisture-sensitive solid (49.6 mg, 0.100 mmol, 31%). ^{1}H NMR (400 MHz, $CDCl_3$): δ = 1.15 (d, J = 6.9 Hz, 6 H, 1-CH(CH_3)$_2$), 1.82 (s, 3 H, 4-CH_3), 2.39 (sept, J = 6.9 Hz, 1 H, 1-CH(CH$_3$)$_2$), 5.03 (dd, J = 8.9, 2.3 Hz, 2 H, 2 × 2″-H$_{cis}$), 5.58 (dd, J = 15.8, 2.3 Hz, 2 H, 2 × 2″-H$_{trans}$), 5.88 (d, J = 6.1 Hz, 2 H, 2-H, 6-H), 5.92 (d, J = 6.1 Hz, 2 H, 3-H, 5-H), 7.05 (dd, J = 15.8, 8.9 Hz, 2 H, 2 × 1″-H), 7.07 (t, J = 1.7 Hz, 2 H, 2 × 4′-H), 7.68 (br s, 2 H, 2 × 5′-H), 9.73 (br s, 2 H, 2 × 2′-H). ^{13}C NMR (100 MHz, $CDCl_3$): δ = 17.93 (4-*C*H$_3$), 22.22

(1-CH(CH_3)$_2$), 30.82 (1-*C*H(CH_3)$_2$), 82.55 (C-2, C-6), 86.04 (C-3, C-5), 100.6 (C-4), 103.6 (C-1), 104.3 (2 × C-2″), 116.0 (2 × C-4′), 129.0 (2 × C-1″), 130.7 (2 × C-5′), 141.0 (2 × C-2′). ESI-MS (MeOH): *m*/*z* (%) = 565.1 (5) [Ru_2(cymene)$_2$(MeOH)$_3$]$^+$, 458.9 (100) [Ru(cymene)(vinylimid)$_2$Cl]$^+$, 367.1 (2) [Ru(cymene)(vinylimid)Cl]$^+$.

[Ru(η^6-*p*-cymene)Cl(imid)$_2$][Cl] (9d). To a suspension of [Ru(η^6-*p*-cymene)Cl$_2$]$_2$ (100 mg, 0.163 mmol) in *i*PrOH (15 mL), imidazole (50.0 mg, 0.734 mmol, 4.50 equiv) was added at room temperature. The resulting mixture was heated to reflux for 8 h. After the mixture was cooled, the solution was decanted from some precipitate, and the solvent was removed in vacuo. The residue was taken up in CH_2Cl_2, and an excess of EE was added. CH_2Cl_2 was removed in vacuo. The obtained turbid solution was kept standing under N_2 at room temperature for 1.5 days. The supernatant was decanted, and the formed precipitate was dried in vacuo, affording a very hygroscopic yellow solid (63.7 mg, 0.144 mmol, 44%). ^{1}H NMR (400 MHz, $CDCl_3$): δ = 1.21 (d, J = 6.5 Hz, 6 H, 1-CH(C*H*$_3$)$_2$), 1.72 (s, 3 H, 4-C*H*$_3$), 2.42 (sept, J = 6.5 Hz, 1 H, 1-C*H*(CH$_3$)$_2$), 5.61 (d, J = 6.0 Hz, 2 H, 2-H, 6-H), 5.71 (d, J = 6.0 Hz, 2 H, 3-H, 5-H), 6.92 (br s, 2 H, 2 × 4′-H), 7.32 (br s, 2 H, 2 × 5′-H), 8.28 (br s, 2 H, 2 × 2′-H); NH not detected. ^{13}C NMR (100 MHz, $CDCl_3$): δ = 17.77 (4-*C*H$_3$), 22.22 (1-CH(*C*H$_3$)$_2$), 30.69 (1-*C*H(CH$_3$)$_2$), 81.61 (C-2, C-6), 85.05 (C-3, C-5), 100.4 (C-4), 103.2 (C-1), 117.1 (2 × C-4′), 129.5 (2 × C-5′), 138.8 (2 × C-2′). ESI-MS (MeOH): *m*/*z* (%) = 406.8 (100) [Ru(cymene)(imid)$_2$Cl]$^+$.

[Ru(η^6-benzene)Cl(imid)$_2$][BPh$_4$] (9e). To a suspension of [Ru(η^6-benzene)Cl$_2$]$_2$ (100 mg, 0.200 mmol) and imidazole (85.0 mg, 1.25 mmol, 6.24 equiv) in acetone (15 mL), $NaBPh_4$ (300 mg, 0.877 mmol, 4.38 equiv) was added at room temperature. The resulting brown suspension was heated to reflux for 4 h. Still slightly warm, the resulting gray-green suspension containing some light-brown solid was filtered over a short pad of Celite. The filter cake was washed with acetone (4 × 20 mL), *i*PrOH (2 × 20 mL), and acetone (20 mL). The combined filtrates were reduced in vacuo to a volume of approximately 6−7 mL. A dark-yellow to brown precipitate began to form. The solution was stored at −25 °C for 20 min to accomplish crystallization. The formed precipitate was filtered with suction, washed with *i*PrOH (2 × 5 mL), and dried in vacuo, affording a dark-yellow crystalline solid (132 mg, 0.197 mmol, 49%). Crystals suitable for X-ray analysis were obtained from acetone/*i*PrOH by slow evaporation. Higher quality crystals were obtained by carefully layering an acetone solution of the compound with Et_2O. ^{1}H NMR (400 MHz, acetone-d_6): δ = 5.91 (s, 6 H, 1-H − 6-H), 6.78 (br t, J = 7.3 Hz, 4 H, 4 × para-H {BPh_4}), 6.92 (t, J = 7.4 Hz, 8 H, 8 × meta-H {BPh_4}), 7.26 (t, J = 1.4 Hz, 2 H, 2 × 4′-H), 7.29−7.36 (br m, 10 H, 2 × 5′-H, 8 × ortho-H {BPh_4}), 8.03 (br s, 2 H, 2 × 2′-H); NH not detected. ^{13}C NMR (100 MHz, acetone-d_6): δ = 86.13 (C-1 to C-6), 118.5 (2 × C-4′), 122.3 (4 × para-C {BPh_4}), 125.3 (q, J_{CB} = 2.8 Hz, 8 × meta-C {BPh_4}), 131.5 (2 × C-5′), 137.0 (q, J_{CB} = 1.4 Hz, 8 × ortho-C {BPh_4}), 139.8 (2 × C-2′), 164.9 (q, J_{CB} = 49.4 Hz, 4 × ipso-C {BPh_4}). ESI-MS (MeOH): *m*/*z* (%) = 406.8 (100) [Ru(cymene)(imid)$_2$Cl]$^+$.

[Ru(η^6-*p*-cymene)(mimid)$_3$][BF$_4$]$_2$ (10a). To a suspension of [Ru(η^6-*p*-cymene)Cl$_2$]$_2$ (100 mg, 0.163 mmol) in MeOH (10 mL), *N*-methylimidazole (80 μL, 1.0 mmol, 6.2 equiv) and $AgBF_4$ (128 mg, 0.658 mmol, 4.03 equiv) were added at room temperature. The resulting mixture was stirred at room temperature in the dark for 2 h and then filtered over a short pad of Celite. The filter cake was washed with MeOH (5 × 15 mL). The collected filtrates were evaporated in vacuo to a volume of approximately 10 mL. EE (30 mL) was added, and the solvent was then removed in vacuo until the beginning of crystallization. After standing at room temperature for 1 h, the formed crystals were filtered with suction, washed with EE (2 × 5 mL), and dried in vacuo, affording an intensive yellow crystalline solid (124 mg, 0.189 mmol, 58%). Crystals suitable for X-ray analysis were obtained by slow crystallization from MeOH/EE. ^{1}H NMR (400 MHz, acetone-d_6): δ = 1.12 (d, J = 6.9 Hz, 6 H, 1-CH(C*H*$_3$)$_2$), 1.83 (s, 3 H, 4-C*H*$_3$), 2.45 (sept, J = 6.9 Hz, 1 H, 1-C*H*(CH$_3$)$_2$), 3.85 (s, 9 H, 3 × 1″-H$_3$), 5.95 (d, J = 6.2 Hz, 2 H, 2-H, 6-H), 6.21 (d, J = 6.2 Hz, 2 H, 3-H, 5-H), 6.68 (t, J = 1.3 Hz, 3 H, 3 × 4′-H), 7.34 (t, J = 1.3 Hz, 3 H, 3 × 5′-H), 8.19 (br s, 3 H, 3 × 2′-H). ^{13}C NMR (100 MHz, acetone-d_6): δ = 17.89 (4-*C*H$_3$), 22.43 (1-CH(*C*H$_3$)$_2$), 31.18 (1-*C*H(CH$_3$)$_2$), 35.08 (3 × C-1″), 84.12 (C-2, C-6), 87.82 (C-3, C-5), 104.5 (C-4), 106.2 (C-1), 123.7 (3 × C-4′), 131.7 (3 × C-5′), 143.5 (3 × C-2′). ESI-MS (CH_3CN): *m*/*z* (%) = 568.9 (50) [Ru(cymene)(mimid)$_3$(BF$_4$)]$^+$, 240.9 (100) [Ru(cymene)(mimid)$_3$]$^{2+}$.

[Ru(η^6-benzene)(mimid)$_3$][BF$_4$]$_2$ (10b). To a suspension of [Ru(η^6-benzene)Cl$_2$]$_2$ (100 mg, 0.200 mmol) in $CHCl_3$ (10 mL), *N*-methylimidazole (110 μL, 1.39 mmol, 6.93 equiv) and $AgBF_4$ (164 mg, 0.842 mmol, 4.21 equiv) were added at room temperature. The resulting mixture was stirred at room temperature in the dark for 2 h and then filtered over a short pad of Celite. The filter cake was washed with $CHCl_3$ (2 × 10 mL) and MeOH (4 × 10 mL). The collected filtrates were evaporated in vacuo. The residue was taken up in EE (30 mL) and CH_2Cl_2 (15 mL). The mixture was stirred at 40 °C for 10 min, and CH_2Cl_2 was removed in vacuo. The yellow EE solution was decanted from some insoluble slimy precipitate. The residue was extracted again with EE (20 mL) at room temperature. The combined extracts were concentrated in vacuo until strong crystallization set in. The precipitate was filtered, washed with EE (2 × 5 mL), and dried in vacuo, affording a gray-yellow crystalline solid (52.2 mg, 87.1 μmol, 22%). Crystals suitable for X-ray analysis were obtained by slow crystallization from MeOH/EE. ^{1}H NMR (400 MHz, acetone-d_6): δ = 3.82 (s, 9 H, 3 × 1″-H$_3$), 6.22 (s, 6 H, 1-H − 6-H), 6.71 (t, J = 1.4 Hz, 3 H, 3 × 4′-H), 7.36 (t, J = 1.4 Hz, 3 H, 3 × 5′-H), 8.01 (br s, 3 H, 3 × 2′-H). ^{13}C NMR (100 MHz, acetone-d_6): δ = 35.13 (3 × C-1″), 87.99 (C-1 − C-6), 123.8 (3 × C-4′), 131.6 (3 × C-5′), 143.2 (3 × C-2′). ESI-MS (CH_3CN): *m*/*z* (%) = 512.9 (18) [Ru(benzene)(mimid)$_3$(BF$_4$)]$^+$, 212.9 (100) [Ru(benzene)(mimid)$_3$]$^{2+}$, 192.4 (39) [Ru(benzene)(mimid)$_2$(CH_3CN)]$^{2+}$.

Single-Crystal X-ray Analysis. Crystals suitable for analysis by X-ray diffraction were coated with hydrocarbon oil and mounted on the end of a thin glass fiber, and the crystal was immersed in a rapid stream of low-temperature N_2. The primary and cell reflection data were collected using either a Bruker Kappa/Apex II or Oxford Diffraction KM4/sapphire diffractometer, both equipped with graphite monochromated Mo Kα radiation and a CCD detector. Standard reflections were continuously monitored for crystal deterioration; none of the samples demonstrated any form of decay. Cell parameters and space group determination were performed using the program Dirax[44] or CrysAlis CCD[45] by Oxford Diffraction. Reflection data was processed using EvalCCD[46] or CrysAlis RED[45] software, and absorption correction based on the multiscan method was obtained through the SADABS[47] program. Structure solutions were obtained using SIR92[48] or SHELXS;[49] in both cases a direct method algorithm was employed. Structure refinement using SHELXL[49] involved continuous cycles of full matrix least-squares refinement on F^2. All non-hydrogen atoms were refined anisotropically; hydrogens atoms with strong data were located, but most were placed in geometry calculated positions and refined with a riding model. Graphical representation of the structure was made with ORTEP-3.[50] Hydrogens bonded to water were fixed according to standard bond lengths. The important crystallographic parameters for each structure are given in Table S1 in Supporting Information.

In Vitro Tests. TS/A murine adenocarcinoma cell lines, initially obtained from Dr. G. Forni (CNR, Centro di Immunogenetica ed Oncologia Sperimentale, Torino, Italy), belong to the tumor cell panel of the Callerio Foundation and are stored in liquid nitrogen. Cells were cultured according to a standard procedure[51] and maintained in RPMI-1640 medium (EuroClone, Wetherby, U.K.) supplemented with 10% fetal bovine serum (FBS, Invitrogen, Milano, Italy), 2 mM L-glutamine (EuroClone, Wetherby, U.K.), and 50 μg/mL gentamycin sulfate solution (EuroClone, Wetherby, U.K.). The cell line was kept in a CO_2 incubator with 5% CO_2 and 100% relative humidity at 37 °C. Cells from a confluent monolayer were removed from flasks by a trypsin−EDTA solution (EuroClone, Wetherby, U.K.).

HBL-100 nontumorigenic human breast cells obtained from ATCC (American Type Culture Collection) were maintained in McCoy's 5A medium (Sigma, St. Louis, MO) supplemented with 10% FBS, 2 mM L-glutamine, 100 UI/mL penicillin, and 100 μg/mL streptomycin (EuroClone, Whetherby, U.K.) in a humidified atmosphere with 5% CO_2 at 37 °C.

Cell viability was determined by the trypan blue dye exclusion test. For experimental purposes, the cells were sown in multiwell cell culture plastic plates (Corning Costar Italia, Milano, Italy). Cell growth was determined by the MTT viability test.[52] Cells were sown on 96-well plates and 24 h after were incubated with the appropriate compound at 1−300 μM, prepared by dissolving in a medium containing 5% of serum for 24, 48, and 72 h. Analysis was performed at the end of the incubation time. Briefly, MTT [3-(4,5-dimethylthiazol-2-yl)-2,5-diphenyltetrazolium bromide] dissolved in PBS (5 mg/mL) was added (10 μL per 100 μL of medium) to all wells, and the plates were then incubated at 37 °C with 5% CO_2 and 100% relative humidity for 4 h. After this time, the medium was discarded and 100 μL of DMSO (Sigma, St. Louis, MO) was added to each well according to the method of Alley et al.[53] Optical density was measured at 570 nm on a SpectraCount Packard (Meriden, CT) instrument. Graphs indicating the cytotoxic effects of **8a**−**c**, **9b**,**c**, and **10a**,**10b** on TS/A and HBL-100 cells are provided in Figure S1 of Supporting Information.

Acknowledgment. We thank the Swiss National Science Foundation, the EPFL, COST (Switzerland), LINFA Laboratories, and CRTrieste Foundation for financial support. A postdoc stipend provided from the German Academic Exchange Service (DAAD) for C.A.V. is gratefully acknowledged.

Supporting Information Available: Crystallographic data in CIF format, structures for all synthesized compounds with numbering schemes for NMR assignments, elemental analysis results, crystallographic parameters, and cell viability studies. This material is available free of charge via the Internet at http://pubs.acs.org.

References

(1) Rosenberg, B.; Vancamp, L.; Krigas, T. Inhibition of cell division in *Escherichia coli* by electrolysis products from a platinum electrode. *Nature* **1965**, *205*, 698−699.
(2) Rosenberg, B.; Vancamp, L.; Trosko, J. E.; Mansour, V. H. Platinum compounds: a new class of potent antitumour agents. *Nature* **1969**, *222*, 385.
(3) Allardyce, C. S.; Dyson, P. J. Ruthenium in medicine: current clinical uses and future prospects. *Platinum Met. Rev.* **2001**, *45*, 62−69.
(4) Cocchietto, M.; Sava, G. Blood concentration and toxicity of the antimetastasis agent NAMI-A following repeated intravenous treatment in mice. *Pharmacol. Toxicol.* **2000**, *87*, 193−197.
(5) Zorzet, S.; Sorc, A.; Casarsa, C.; Cocchietto, M.; Sava, G. Pharmocological effects of the ruthenium complex NAMI-A given orally to CBA mice with MCa mammary carcinoma. *Met.-Based Drugs* **2001**, *8*, 1−7.
(6) Sava, G.; Bergamo, A. Ruthenium-based compounds and tumour growth control (review). *Int. J. Oncol.* **2000**, *17*, 353−365.
(7) Gagliardi, R.; Sava, G.; Pacor, S.; Mestroni, G.; Alessio, E. Antimetastatic action and toxicity on healthy tissues of Na-[trans-$RuCl_4$(DMSO)Im] in the mouse. *Clin. Exp. Metastasis* **1994**, *12*, 93−100.
(8) Magnarin, M.; Bergamo, A.; Carotenuto, M. E.; Zorzet, S.; Sava, G. Increase of tumour-infiltrating lymphocytes in mice treated with antimetastatic doses of NAMI-A. *Anticancer Res.* **2000**, *20*, 2939−2944.
(9) Rademaker-Lakhai, J. M.; Van den Bongard, D.; Pluim, D.; Beijnen, J. H.; Schellens, J. H. A phase I and pharmacological study with imidazolium-trans-DMSO-imidazole-tetrachlororuthenate, a novel ruthenium anticancer agent. *Clin. Cancer Res.* **2004**, *10*, 3717−3727.
(10) Sava, G.; Frausin, F.; Cocchietto, M.; Vita, F.; Podda, E.; Spessotto, P.; Furlani, A.; Scarcia, V.; Zabucchi, G. Actin-dependent tumour cell adhesion after short-term exposure to the anti-metastasis ruthenium complex NAMI-A. *Eur. J. Cancer* **2004**, *40*, 1383−1396.
(11) Zorzet, S.; Bergamo, A.; Cocchietto, M.; Sorc, A.; Gava, B.; Alessio, E.; Iengo, E.; Sava, G. Lack of in vitro cytotoxicity, associated to increased G(2)-M cell fraction and inhibition of Matrigel invasion, may predict in vivo-selective antimetastasis activity of ruthenium complexes. *J. Pharmacol. Exp. Ther.* **2000**, *295*, 927−933.
(12) Gava, B.; Zorzet, S.; Spessotto, P.; Cocchietto, M.; Sava, G. Inhibition of B16 melanoma metastases with the ruthenium complex imidazolium trans-imidazoledimethylsulfoxide-tetrachlororuthenate and down-regulation of tumor cell invasion. *J. Pharmacol. Exp. Ther.* **2006**, *317*, 284−291.
(13) Sava, G.; Zorzet, S.; Turrin, C.; Vita, F.; Soranzo, M.; Zabucchi, G.; Cocchietto, M.; Bergamo, A.; DiGiovine, S.; Pezzoni, G.; Sartor, L.; Garbisa, S. Dual action of NAMI-A in inhibition of solid tumor metastasis: Selective targeting of metastatic cells and binding to collagen. *Clin. Cancer Res.* **2003**, *9*, 1898−1905.
(14) Vacca, A.; Bruno, M.; Boccarelli, A.; Coluccia, M.; Ribatti, D.; Bergamo, A.; Garbisa, S.; Sartor, L.; Sava, G. Inhibition of endothelial cell functions and of angiogenesis by the metastasis inhibitor NAMI-A. *Br. J. Cancer* **2002**, *86*, 993−998.
(15) Seelig, M. H.; Berger, M. R.; Keppler, B. K. Antineoplastic activity of three ruthenium derivatives against chemically induced colorectal carcinoma in rats. *J. Cancer. Res. Clin. Oncol.* **1992**, *118*, 195−200.
(16) Jakupec, M. A.; Arion, V. B.; Kapitza, S.; Reisner, E.; Eichinger, A.; Pongratz, M.; Marian, B.; Graf von Keyserlingk, N.; Keppler, B. K. KP1019 (FFC14A) from bench to bedside: preclinical and early clinical development. An overview. *Int. J. Clin. Pharmacol. Ther.* **2005**, *43*, 595−596.
(17) Allardyce, C. S.; Dorcier, A.; Scolaro, C.; Dyson, P. J. Development of organometallic (organo-transition metal) pharmaceuticals. *Appl. Organomet. Chem.* **2005**, *19*, 1−10.
(18) Vessieres, A.; Top, S.; Beck, W.; Hillard, E.; Jaouen, G. Metal complex SERMs (selective oestrogen receptor modulators). The influence of different metal units on breast cancer cell antiproliferative effects. *Dalton Trans.* **2006**, 529−541.
(19) *Bioorganometallics*; Jaouen, G., Ed.; Wiley-VCH: Weinheim, Germany, 2005.
(20) Dale, L. D.; Tocher, J. H.; Dyson, T. M.; Edwards, D. I.; Tocher, D. A. Studies on DNA damage and induction of SOS repair by novel multifunctional bioreducible compounds. II. A metronidazole adduct of a ruthenium-arene compound. *Anti-Cancer Drug Des.* **1992**, *7*, 3−14.
(21) Morris, R. E.; Aird, R. E.; del Socorro Murdoch, P.; Chen, H.; Cummings, J.; Hughes, N. D.; Parsons, S.; Parkin, A.; Boyd, G.; Jodrell, D. I.; Sadler, P. J. Inhibition of cancer cell growth by ruthenium(II) arene complexes. *J. Med. Chem.* **2001**, *44*, 3616−3621.
(22) Allardyce, C. S.; Dyson, P. J.; Ellis, D. J.; Heath, S. L. [Ru(η^6-*p*-cymene)Cl_2(pta)] (pta = 1,3,5-triaza-7-phosphatricyclo[3.3.1.1]-decane: a water soluble compound that exhibits pH dependent DNA binding providing selectivity for diseased cells. *Chem. Commun.* **2001**, 1396−1397.
(23) Scolaro, C.; Bergamo, A.; Brescacin, L.; Delfino, R.; Cocchietto, M.; Laurenczy, G.; Geldbach, T. J.; Sava, G.; Dyson, P. J. In vitro and in vivo evaluation of ruthenium(II)-arene PTA complexes. *J. Med. Chem.* **2005**, *48*, 4161−4171.
(24) Dorcier, A.; Dyson, P. J.; Gossens, C.; Rothlisberger, U.; Scopelliti, R.; Tavernelli, I. Binding of organometallic ruthenium(II) and osmium(II) complexes to an oligo-nucleotide: a combined mass spectrometric and theoretical study. *Organometallics* **2005**, *24*, 2114−2123.
(25) Scolaro, C.; Geldbach, T. J.; Rochat, S.; Dorcier, A.; Gossens, C.; Bergamo, A.; Cocchietto, M.; Tavernelli, I.; Sava, G.; Rothlisberger, U.; Dyson, P. J. Influence of hydrogen-bonding substituents on the cytotoxicity of RAPTA compounds. *Organometallics* **2006**, *25*, 756−765.
(26) Serli, B.; Zangrando, E.; Gianferrara, T.; Scolaro, C.; Dyson, P. J.; Bergamo, A.; Alessio, E. Is the aromatic fragment of piano-stool ruthenium compounds an essential feature for anticancer activity? The development of new Ru^{II}-[9]aneS_3 analogues. *Eur. J. Inorg. Chem.* **2005**, 3423−3434.
(27) Pandey, D. S.; Sahay, A. N.; Agarwala, U. C. Synthesis and characterisation of [Ru(η^6-C_6Me_6)Cl_2(CNPy)] and [Cl_2(η^6-C_6Me_6)-Ru(μ-CNPy)Ru(η^6-C_6Me_6)Cl_2] and reactivity of [Ru(η^6-C_6Me_6)Cl_2-(CNPy)] with various bases. *Indian J. Chem.* **1996**, *A35*, 434−437.
(28) Singh, S. K.; Trivedi, M.; Chandra, M.; Sahay, A. N.; Pandey, D. S. Luminiscent piano-stool complexes incorporating 1-(4-cyanophenyl)-imidazole: synthesis, spectral and structural studies. *Inorg. Chem.* **2004**, *43*, 8600−8608.
(29) Bennett, M. A.; Smith, A. K. Arene ruthenium(II) complexes formed by dehydrogenation of cyclohexadienes with ruthenium(III) trichloride. *J. Chem. Soc., Dalton Trans.* **1974**, 233−241.
(30) Zaramella, S.; Strömberg, R.; Yeheskiely, E. Stability studies of *N*-acylimidazoles. *Eur. J. Org. Chem.* **2002**, 2633−2639.
(31) Cabeza, J. A.; da Silva, I.; del Rio, I.; Garcia-Granda, S. [*N*,*N*′-Bis-(6-methylpyrid-2-ylium)-(1*R*,2*R*)-1,2-diaminocyclohexane] bis-[(*p*-cymene)-trichlororuthenate(II)]. *Appl. Organomet. Chem.* **2005**, *19*, 209−210.

(32) Robertson, D. R.; Stephenson, T. A. Cationic and anionic complexes of ruthenium(II) containing η^6-arene ligands. *J. Organomet. Chem.* **1976**, *116*, C29−C30.
(33) Robertson, D. R.; Stephenson, T. A.; Arthur, T. Cationic, neutral and anionic complexes of ruthenium(II) containing η^6-arene ligands. *J. Organomet. Chem.* **1978**, *162*, 121−136.
(34) Standfest-Hauser, C. M.; Schmid, R.; Kirchner, K.; Mereiter, K. Formation of a hydroxo-bridged dinuclear Ru(III)/Ru(III) complex from *N*-methylimidazole and $[RuCp(CH_3CN)_3]^+$. *Monatsh. Chem.* **2004**, *135*, 911−917.
(35) Caballero, A.; Jalon, F. A.; Manzano, B. R.; Espino, G.; Perez-Manrique, M.; Mucientes, A.; Poblete, F. J.; Maestro, M. Ruthenium arene derivatives with PN hemilabile ligands. P−C cleavage and phosphine to phosphinate transformation. *Organometallics* **2004**, *23*, 5694−5706.
(36) Crystallographic data for the structures in this paper have been deposited with the Cambridge Crystallographic Data Centre as supplementary publications CCDC 604182−604186. Copies of the data can be obtained, free of charge, on application to CCDC, 12 Union Road, Cambridge CB2 1EZ, U.K. (fax, +44 1223 336033; e-mail, deposit@ccdc.cam.ac.uk).
(37) Kiviniemi, S.; Nissinen, M.; Alaviuhkola, T.; Rissanen, K.; Pursiainen, J. The complexation of tetraphenylborate with organic N-heteroaromatic cations. *J. Chem. Soc., Perkin Trans. 2* **2001**, 2364.
(38) Keppler, B. K.; Henn, M.; Juhl, U. M.; Berger, M. R.; Niebl, R.; Wagner, F. E. New ruthenium complexes for the treatment of cancer. *Prog. Clin. Biochem. Med.* **1989**, *10*, 41−69.
(39) Yan, Y. K.; Melchart, M.; Habtemariam, A.; Sadler, P. J. Organometallic chemistry, biology and medicine: ruthenium arene anticancer complexes. *Chem. Commun.* **2005**, 4764−4776.
(40) Aird, R. E.; Cummings, J.; Ritchie, A. A.; Muir, M.; Morris, R. E.; Chen, H.; Sadler, P. J.; Jodrell, D. I. In vitro and in vivo activity and cross resistance profiles of novel ruthenium(II) organometallic arene complexes in human ovarian cancer. *Br. J. Cancer* **2002**, *86*, 1652−1657.
(41) Bennett, M. A.; Huang, T.-N.; Matheson, T. W.; Smith, A. K. (η^6-Hexamethylbenzene)-ruthenium complexes. *Inorg. Synth.* **1982**, *21*, 74−78.
(42) Gottlieb, H. E.; Kotlyar, V.; Nudelman, A. NMR chemical shifts of common laboratory solvents as trace impurities. *J. Org. Chem.* **1997**, *62*, 7512−7515.
(43) Dyson, P. J.; McIndoe, J. S. Analysis of organometallic compounds using ion trap mass spectrometry. *Inorg. Chim. Acta* **2003**, *354*, 68−74.
(44) Duisenberg, A. J. M. Indexing in single-crystal diffractometry with an obstinate list of reflections. *J. Appl. Crystallogr.* **1992**, *25*, 92−96.
(45) *CrysAlis CCD*, version 1.170, and *CrysAlis RED*, version 1.170.; Oxford Diffraction Ltd., Abingdon, Oxfordshire, U.K., 2003.
(46) Duisenberg, A. J. M.; Kroon-Batenburg, L. M. J.; Schreurs, A. M. M. An intensity evaluation method: EVAL-14. *J. Appl. Crystallogr.* **2003**, *36*, 220−229.
(47) Sheldrick, G. M. *SADABS. Program for Empirical Absorption Correction of Area Detector Data*; University of Göttingen: Göttingen, Germany, 1996.
(48) Altomare, A.; Cascarano, G.; Giacovazzo, C.; Guagliardi, A.; Burla, M. C.; Polidori, G.; Camalli, M. SIR92, a program for automatic solution of crystal structures by direct methods. *J. Appl. Crystallogr.* **1994**, *27*, 435.
(49) Sheldrick, G. M. *SHELXS97* and *SHELXL97*; University of Göttingen: Göttingen, Germany, 1997.
(50) Farrugia, L. J. ORTEP-3 for Windows, a version of ORTEP-III with a graphical user interface (GUI). *J. Appl. Crystallogr.* **1997**, *30*, 565.
(51) Nanni, P.; De Giovanni, C.; Lollini, P. L.; Nicoletti, G.; Prodi, G. TS/A: a new metastasising cell line from BALB/c spontaneous mammary adenocarcinoma. *Clin. Exp. Metastasis* **1983**, *1*, 373−385.
(52) Mosmann, T. Rapid colorimetric assay for cellular growth and survival: application to proliferation and cytotoxicity assays. *J. Immunol. Methods* **1983**, *65*, 55−63.
(53) Alley, M. C.; Scudiero, D. A.; Monks, A.; Hursey, M. L.; Czerwinski, M. J.; Fine, D. L.; Abbott, B. J.; Mayo, J. G.; Shoemaker, R. H.; Boyd, M. R. Feasibility of drug screening with panels of human tumor cell lines using a microculture tetrazolium assay. *Cancer Res.* **1988**, *48*, 589−601.

JM060495O